Colloid Polym Sci (2014) 292:1657–1664
DOI 10.1007/s00396-014-3225-9

ORIGINAL CONTRIBUTION

Aggregation behavior of pH- and thermo-responsive block copolymer protected gold nanoparticles

Junbo Li · Wenlan Wu · Chen Han · Shijie Zhang · Huiyun Zhou · Jinwu Guo

Received: 29 December 2013 / Accepted: 3 April 2014 / Published online: 29 April 2014

Abstract Two distinctive block copolymers protected gold nanoparticles (AuNPs) were prepared with poly(methylacrylic acid)-block-poly(*N*-isopropylacrylamide) (SH-PMAA$_{64}$-*b*-PNIPAM$_{35}$) and poly (*N*-isopropylacrylamide)-block-poly(methylacrylic acid) (SH-PNIPAM$_{40}$-*b*- PMAA$_{60}$) through strong gold-sulfur bonding. The hybrid NPs have a pH-responsive inner shell (or corona) and a thermo-responsive corona (or inner shell) due to different location relations of the PNIPAM and PMAA on the surface of AuNPs. Then, the aggregation behaviors, as well as the changes of optical properties, of two hybrid NPs were compared in response to both stimuli. The results showed the obvious inter-particle aggregation caused by the phase transition for hydrophobic coronal polymer. However, the particles of hydrophilic corona layer retained good dispersion and the pH-responsive or thermo-responsive characteristics of shell layer made relatively minor changes.

Keywords The block copolymers · Dual stimuli-responsive · Gold nanoparticles · Aggregation behaviors

Introduction

Gold nanoparticles (AuNPs) have attracted significant interests for their optical, electronic, and biocompatible properties coupled with the ability to parametrically control particle size [1]. The properties of AuNPs could be modified via effective molecular design on their surface, thereby distinguishing them from the corresponding large-sized materials or particles. It has been reported that the organic molecule or macromolecular functionalized AuNPs provide versatile vehicles for a variety of perspective applications in green-catalysis [2–7], cancer therapy [8, 9], drug delivery [10, 11], molecular imaging and sensors [12, 13], etc.

The polymers protected AuNPs is the covalent bonding polymers on the surface of AuNPs to form the core-shell composite. The polymer shells were widely believed to enhance solubilities and introduce functionalities to AuNPs due to the intriguing properties of polymer [14–17]. The covalent bonding can be easily achieved through the techniques of "grafting to" approach. The "grafting to" approach was firstly synthesized polymers with a thiol terminal group and then grafted polymers onto AuNPs via a strong binding affinity between gold and thiol ending. The well-defined polymers synthesized by reversible addition fragmentation chain transfer (RAFT) have been shown that their dithioester or trithiocarbonate end-groups could be easily converted to thiols, then obtain homopolymers or block copolymer protected AuNPs [18, 19]. Based on the "grafting to" approach, it is interesting that a "smart polymer" will endow AuNPs the stimuli-responsive performance. The properties of stimuli-responsive AuNPs could be easily tuned by changing external condition including temperature, pH value, ionic strength and light, etc. [20–24]. Poly (*N*-isopropylacrylamide) (PNIPAM) and poly (methacrylic acid) (PMAA) are widespread used polymers for relative investigation. Exhibiting a lower critical solution temperature (LCST), PNIPAM is a suitable thermo-responsive polymer for the fabrication of AuNPs [25, 26]. And it is also known that PMAA can undergo notable pH-responsive conformational changes [27, 28].

Moreover, the block copolymers protected AuNPs had a micelle-like three-layer microstructure, consisting of gold core, polymer inner shell and the outer corona. Utilizing the

Electronic supplementary material The online version of this article (doi:10.1007/s00396-014-3225-9) contains supplementary material, which is available to authorized users.

J. Li (✉) · W. Wu · C. Han · S. Zhang · H. Zhou · J. Guo
College of Chemical Engineering & Pharmaceutics, Henan University of Science & Technology, Luo Yang 471023, Henan, China
e-mail: lijunbo@haust.edu.cn

different property and function of each micro zone, the new hierarchical functional materials via the self-assembly of polymer shells was reported and applied in the bioimaging and photothermal therapy of cancer [29]. Besides, the three-layer microstructure have also been designed as the tumor-targeted and controllable release drug delivery carries, where the inner shell used to entrap drugs and outer corona provide stability [30]. For example, Hamner et al. reported that DNA-mediated assembly and encoded nanocarrier drug release could be regulated by thermo-responsive PNIPAAM-*b*-PMAA protected AuNPs [31].

Anyway, the colloidal stability of the hybrid particles is usually the first considered factor in better applications. In fact, the colloidal stability and the function of the particles are always influenced by the changed properties or parameters on the surface polymer [32]. For instance, the microstructure with shell cross-linking can exhibit higher colloidal stability, and the thermo-responsive behavior of block copolymers protected AuNPs can be achieved by adjusting the chain length. Exploring the relationship between colloidal stability and properties of polymer is still a challenge in constructing new hybrid materials or drug delivery carries [33]. Especially for the microstructure with a dual-stimuli response layer, the properties of inner and outer zone are important for the colloidal stability. However, there has been relatively little investigation of the dual-stimuli with different polymer order in block copolymers bonding to AuNPs.

In this work, two dual-stimuli responsive copolymers, SH-$PMAA_{64}$-*b*-$PNIPAM_{35}$ and SH-$PNIPAM_{40}$-*b*-$PMAA_{60}$ were synthesized by RAFT polymerization, and then attached on AuNPs by "grafting to" approach, that leaving the PMAA and PNIPAM blocks as the inner shells or outer coronas around the particles. Synthesized by citrate reduction, AuNPs of the uniform size were to avoid interference to surface plasmon resonance (SPR) caused by heterogeneous sizes. The properties of the hybrid AuNPs can be modified by varying pH value and temperature of the aqueous dispersions of the particles. The colloidal stability and the aggregation behavior of the hybrid AuNPs may be controlled by the outer corona through adjusting the pH value or temperature. The effect of block position to colloidal stability is illustrated in Scheme 1. In this case, the aim was to find out whether the outer corona may be observed as a shift in the SPR band of the hybrid AuNPs at different environmental conditions and research their controlled aggregation-dispersion transition upon corresponding stimuli.

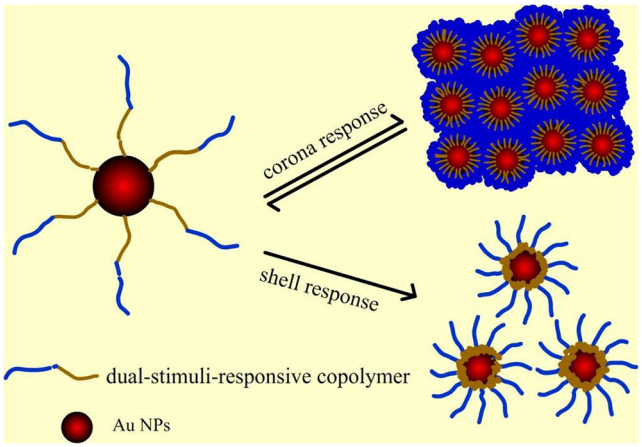

Scheme 1 Schematic illustration of the aggregation behavior of dual stimuli-responsive block copolymers protected AuNPs induced by corona or shell response

Experimental section

Materials Tert-butyl methacrylate (t-BMA) was purchased from Fluka and distilled under vacuum prior to use. 2, 2-Azobis (isobutyronitrile) (AIBN) was purchased from J&K Chemical and recrystallized before as an initiator. *N*-isopropylacryl-amide (NIPAM) was purchased from Aldrich and recrystallized twice from benzene. Dioxane, tetrahydrofuran, and *N*, *N*-dimethylformamide were purchased from National Pharmaceutical Group Chemical Reagent and distilled before use. $HAuCl_4 \cdot 4H_2O$, sodium citrate, and trifluoroacetic acid were purchased from National Pharmaceutical Group Chemical Reagent and used as received. The RAFT agent, 2-(2-cyanopropyl) dithiobenzoate (CPDB) was synthesized according to the literature procedure [34].

Preparation of SH-$PMAA_{64}$-b-$PNIPAM_{35}$ and SH-$PNIPAM_{40}$-b-$PMAA_{60}$ The block copolymers, SH-$PMAA_{64}$-*b*-$PNIPAM_{35}$ and SH-$PNIPAM_{40}$-*b*-$PMAA_{60}$ were prepared by P*t*-BMA-*b*-PNIPAM and PNIPAM-*b*-P*t*-BMA, which were synthesized by two-step RAFT polymerization using CPDB as initial chain transfer agent via different order of feed. The detail process and characterization are shown in support information. Finally, SH-$PMAA_{64}$-*b*-$PNIPAM_{35}$ and SH-$PNIPAM_{40}$-*b*-$PMAA_{60}$ was obtained by the hydrolysis of P*t*-BMA-*b*-PNIPAM and PNIPAM-*b*-P*t*-BMA in the presence of TFA in dry $CHCl_3$.

Preparation of the block copolymers protected AuNPs AuNPs were firstly prepared through the reduction of $HAuCl_4$ by sodium citrate [35]. In brief, 20 mL $HAuCl_4$ (1 g/L) were diluted by 160-ml distilled water, and heated at 100 °C for 5 min under reflux and stirring vigorously. Twenty milliliter sodium citrate solution (38.8 mM) were added rapidly while stirring continuously. The solution was stirred for further 15 min. During that time, the color of solution turned from pale yellow to wine, which indicated AuNPs formed. Then, the solution was cooled to room temperature and the excessive sodium citrate was removed by dialysis. The block copolymers protected AuNPs were prepared by adding 0.01 g

of SH-PMAA$_{64}$-*b*-PNIPAM$_{35}$ and SH-PNIPAM$_{40}$-*b*-PMAA$_{60}$ to the as-prepared AuNPs solution (0.01 wt%) with stirring overnight, respectively. Finally, the mixtures were centrifuged for 5 min at 12,000 rpm, and the depositions were washed three times by distilled water for removing excessive polymers to obtain PMAA-*b*-PNIPAM-@-AuNPs and PNIPAM-*b*-PMAA-@-AuNPs.

Characterization The molecular weight distribution (M_w/M_n) of the polymer was characterized by a Waters 600E gel permeation chromatography (GPC) analysis system equipped with a Waters styragel HT column using poly(ethylene oxide) as the calibration standard and THF as the eluent (flow rate 0.4 mL/min). Dynamic laser scattering (DLS) measurements were performed using a laser light scattering spectrometer (BI-200SM) equipped with a digital correlator (BI-9000AT) at 532 nm at room temperature. Transmission electron microscopy (TEM) measurement was conducted using a JEM-2100 electron microscopy at an acceleration voltage of 200 kV, a small drop of solution was deposited onto a carbon-coated copper EM grid and dried atmospheric pressure. The UV-Vis spectra were recorded on a Cary 50 Bio UV-Visible Spectrophotometer (Varian, USA), equipped with two silicon diode detectors and a xenon flash lamp. ^{1}H NMR spectroscopy was conducted on a Bruker AV300 spectrometer.

Results and discussion

Characterization of the block copolymers protected AuNPs The well-defined polymers synthesized by RAFT have the dithioesters or trithiocarbonate end groups, which can be easily converted to thiols and then obtain polymer protected AuNPs due to the strong affinity between gold and thiol ending [36–38]. In the present study, AuNPs were firstly prepared by reducing chloroauric acid with sodium citrate. The block copolymers protected AuNPs could be achieved in one-step process simply by adding PMAA-*b*-PNIPAM-SH and PNIPAM-*b*-PMAA-SH into an AuNPs aqueous solution. The UV-Vis spectroscopy was used to characterize the grafting block copolymers on the surface of AuNPs based on the increase of refractive index and the red shift in the absorbance spectra. As shown in Fig. 1a, the characteristic SPR band of AuNPs, prepared by citrate reduction, is observed in the spectrum at approximate 521 nm. After addition of the SH-PMAA$_{64}$-*b*-PNIPAM$_{35}$ and SH-PNIPAM$_{40}$-*b*-PMAA$_{60}$, the characteristic SPR band of the hybrid AuNPs is displaced at approximate 526 nm (Fig. 1b) and 530 nm (Fig. 1c). The UV absorption peaks have red shift of 5 and 9 nm. The slight red shift could be attributed to the chemisorption of copolymers on the surface of AuNPs for the copolymer has a higher refractive index compared to that of water [39].

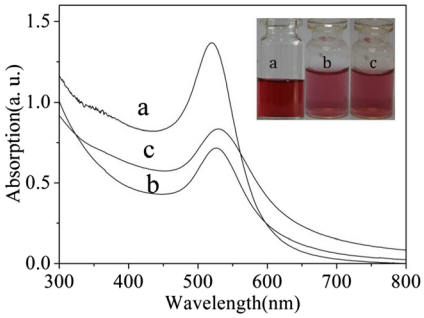

Fig. 1 UV-Vis spectra of AuNPs (**a**), PMAA-*b*-PNIPAM-@-AuNPs (**b**), and PNIPAM-*b*-PMAA-@-AuNPs (**c**), where the concentration of naked AuNP was 0.01 wt%, and the PMAA-*b*-PNIPAM-@-AuNPs and PNIPAM-*b*-PMAA-@-AuNPs were prepared by 0.01 wt% naked AuNP conjugating with 0.01 mmol/L corresponding polymer; measured at pH 7 and 20 °C

The hydrodynamic diameter and distribution of the three AuNPs solutions were measured by DLS. As an example shown in Fig. 2a, the average hydrodynamic diameter (D_h) of the AuNPs is approximately 12 nm and the size distribution range is 9–15 nm. After addition of block copolymers in AuNPs solutions, the mean diameter of as-prepared PMAA-*b*-PNIPAM-@-AuNPs and PNIPAM-*b*-PMAA-@-AuNPs increase to about 40 and 32 nm. The enlargement of the size is caused by grafting the hydrophilic block copolymer to the surface of AuNPs.

The characterization by TEM (Fig. 3) can directly provide the information of size and size distributions of AuNPs and the block copolymers protected AuNPs. From Fig. 3a, the TEM images confirm the uniform size and narrow size distribution of AuNPs with sodium citrate as a reducing and stabilizing agent. Besides, Fig. 3c, e are the TEM images of PMAA-*b*-PNIPAM-@-AuNPs and PNIPAM-*b*-PMAA-@-AuNPs. From Fig. 3c, e, the both hybrid particles are found a good dispersion due to the electrostatic repulsion and steric hindrance of polymers. The typical structures of AuNPs

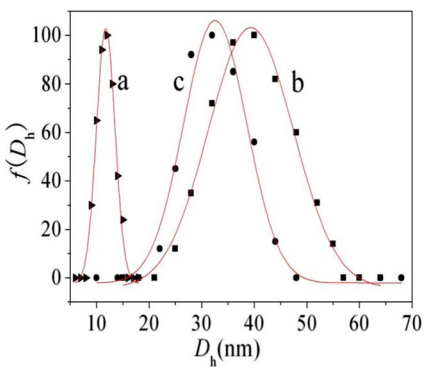

Fig. 2 Hydrodynamic diameter distributions of AuNPs (**a**), PMAA-*b*-PNIPAM-@-AuNPs (**b**), and PNIPAM-*b*-PMAA-@-AuNPs (**c**), where the concentration of naked AuNPs was 0.01 wt%, and the PMAA-*b*-PNIPAM-@-AuNPs and PNIPAM-*b*-PMAA-@-AuNPs were prepared by 0.01 wt% naked AuNPs conjugating with 0.01 mmol/L corresponding polymers; measured at pH 7 and 20 °C

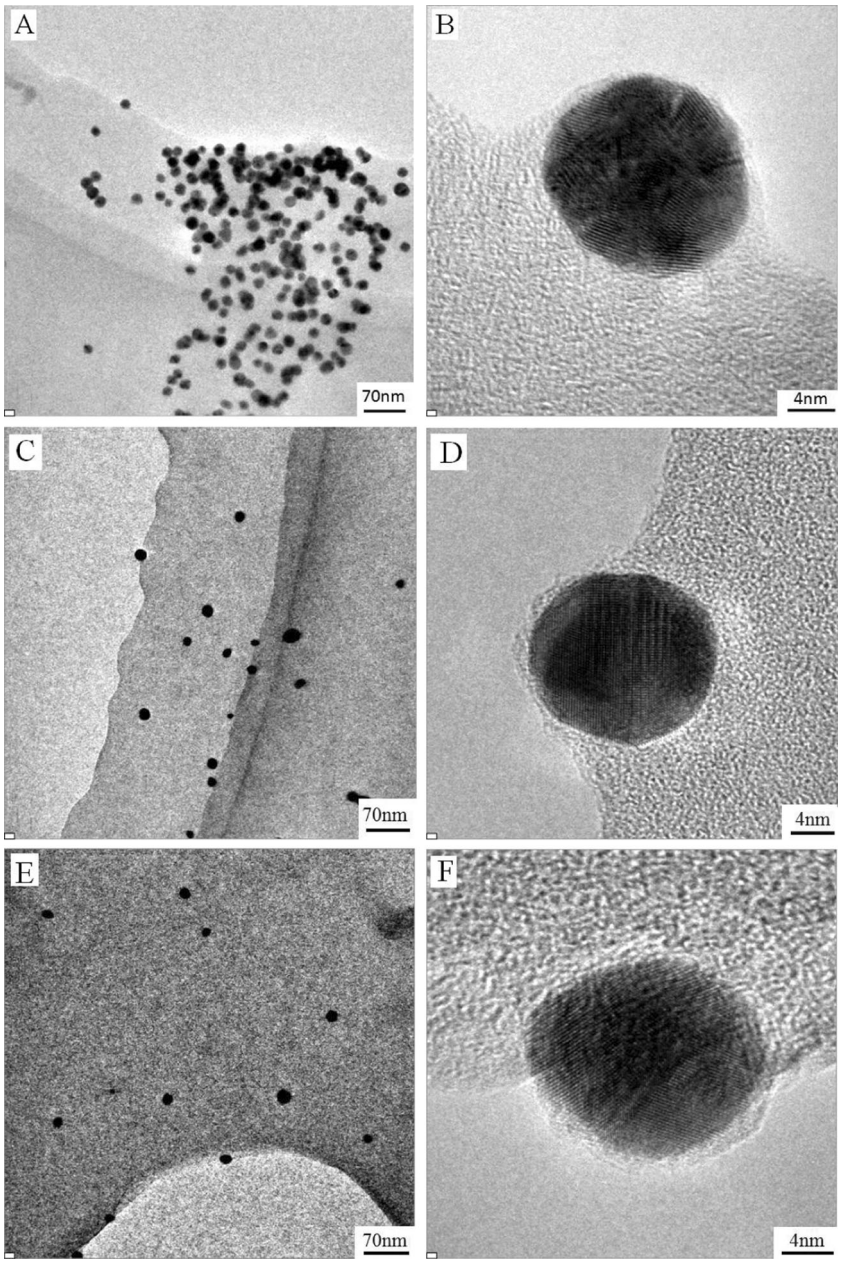

Fig. 3 TEM images of **a** the AuNPs and **b** with the high magnification of **a**, **c** the PMAA-*b*-PNIPAM-@-AuNPs and **d** with the high magnification of **c**, **e** the PNIPAM-*b*-PMAA-@-AuNPs and **f** with the high magnification of **e**

protected by copolymers can be directly observed by contrasting Fig. 3b, d, f, where are magnified single particles in Fig. 3a, c, e, respectively. As shown in Fig. 3b, d, f, the packing of the gold atoms in the clusters forms the crystal

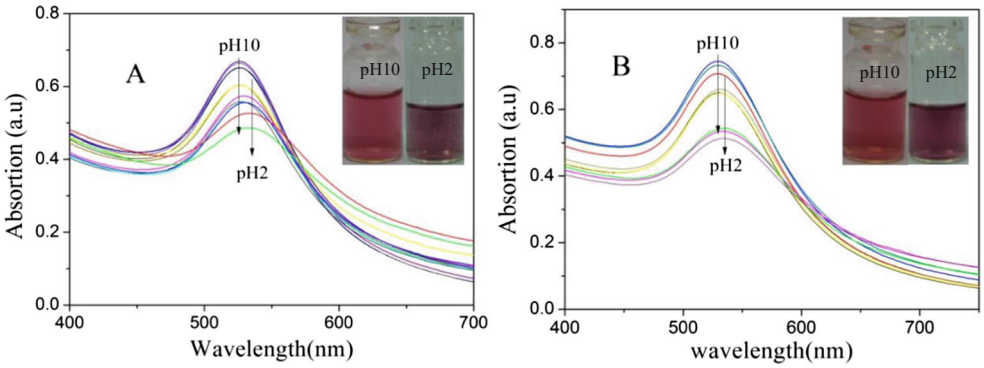

Fig. 4 The UV spectra and color of PMAA-*b*-PNIPAM-@-AuNPs (**a**) and PNIPAM-*b*-PMAA-@-AuNPs (**b**) solution at different pH values. Both hybrid particles were prepared by 0.01 wt% naked AuNPs conjugating with 0.01 mmol/L corresponding polymers and measured at 20 °C

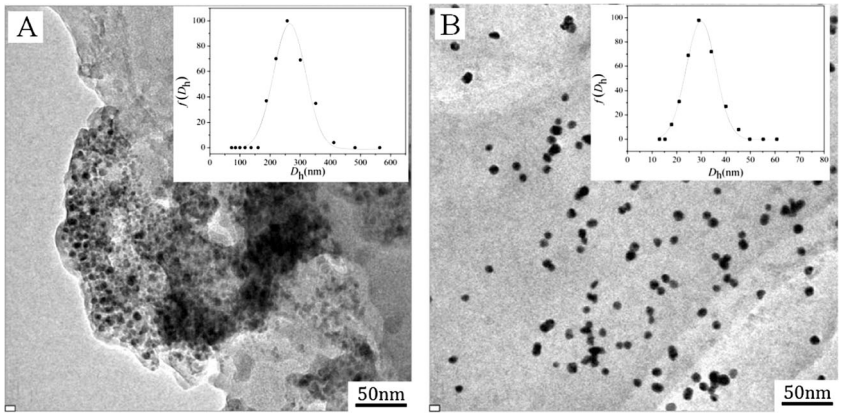

Fig. 5 The TEM images of PMAA-*b*-PNIPAM-@-AuNPs (**a**) and PNIPAM-*b*-PMAA-@-AuNPs (**b**) at pH 3

structure as the core. The existence of the polymer layer around the gold core (Fig. 3d, f) is obviously observed and belongs to amorphous phase of polymer-grafted chains [40]. Because AuNPs have a close package by dual-stimuli responsive block copolymer, the hydrophilic polymer at the periphery of the sphere will not only improve the stability and dispersibility of the particles, but introduce a new function of pH and temperature response.

pH-responsive properties of PMAA-b-PNIPAM-@-AuNPs and PNIPAM-b-PMAA-@-AuNPs It is well known that PMAA can undergo pH-induced conformational transition. At low pH, PMAA chains adopted a compact structure due to hydrophobic interactions. Whereas, the carboxyl groups at high pH, the fully ionized polymers adopted a stretched conformation due to the ionic repulsion [41, 42]. Herein, the pH-responsive PMAA located at the outer corona of PMAA-*b*-PNIPAM-@-AuNPs and inner shell of PNIPAM-*b*-PMAA-@-AuNPs. The influence of pH-induced phase transition on colloidal stability can be compared between different block position combinations.

The UV spectra of the colloids at different pH values were firstly investigated by UV-Vis absorption spectroscopy shown in Fig. 4. From Fig. 4a, the SPR peaks of PMAA-*b*-PNIPAM-@-AuNPs have a little change during the decrease

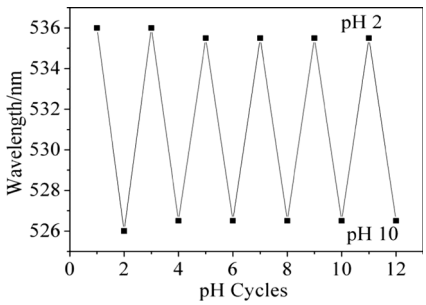

Fig. 6 pH-induced switching of SPR of PMAA-b-PNIPAM-@-AuNPs, where the solution was prepared by 0.01 wt% naked AuNPs conjugating with 0.01 mmol/L PMAA-b-PNIPAM and measured at 20 °C

pH from 10 to 6, but have a sharp redshift as the pH lower than 5. The obvious red shift is found from 526 to 536 nm with increasing the acidity of the solution. Meanwhile, the solution turned from clear and transparent wine red liquid to suspension of purple as the inserted photos in Fig. 4a. However, the SPR peak of the PNIPAM-*b*-PMAA-@-AuNPs solution is found only a 4 nm change from 530 to 534 nm shown in Fig. 4b with the changed color of transparent purple (the inserted photos in Fig. 4b). The peak of SPR is known to depend upon various parameters of the AuNPs, such as particle size, particle shape, surface-capping agents as well as the dielectric property of the surrounding medium [43, 44]. Thus, the emergence of suspended solids and the dramatic redshift of SPR in the solution of PMAA-*b*-PNIPAM-@-AuNPs indicate an interparticle aggregation. Correspondingly, the stable colloidal solution and a minor change of SPR in PNIPAM-*b*-PMAA-@-AuNPs attribute to the protective effects of PNIPAM corona which causes the dielectric property of the surrounding medium around AuNPs.

The TEM images of PMAA-*b*-PNIPAM-@-AuNPs and PNIPAM-*b*-PMAA-@-AuNPs at pH 3, shown in Fig. 5, could present a direct evidence for the conclusion in UV-Vis. In Fig. 5a, almost all the hybrid AuNPs are embedded in polymeric precipitation for the aggregation of PMAA-*b*-PNIPAM-@-AuNPs. From the results of DLS, the inserted image on Fig. 5a, mean diameter of PMAA-*b*-PNIPAM-@-AuNPs at pH 3 is about 248 nm and the particle distribution turns broad (138–421 nm), further confirming that the interparticle aggregation is induced by phase transition of the outer PMAA corona. Whereas, the PNIPAM-*b*-PMAA-@-AuNPs are dispersed well (Fig. 5b). Besides, the shrunk D_h (from 32 to 29 nm) indicates the particles are stabilize by the outer PNIPAM corona although the inner PMAA chains collapse on the surface of AuNPs.

After reversed pH to 10.0, the aggregated PMAA-*b*-PNIPAM-@-AuNPs were found redissolved in solution and those SPR recovered. The reversible variations of SPR are repeatedly cycled between pH 2.0 and 10.0, as shown in Fig. 6. With the pH switching between 2.0 and 10.0, the

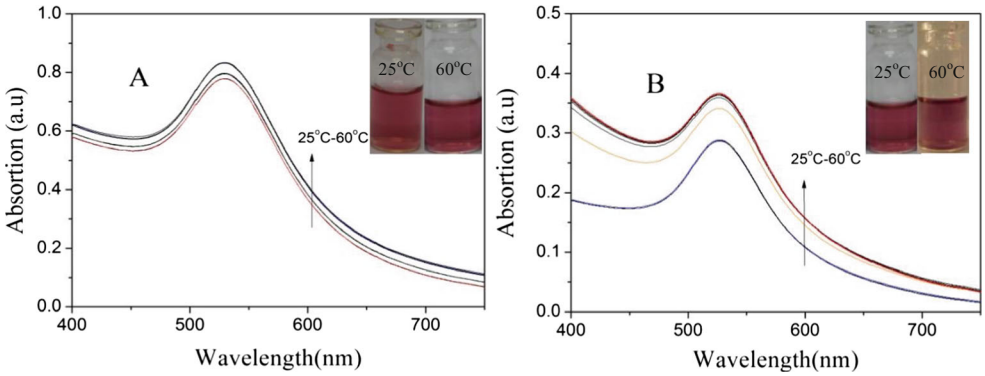

Fig. 7 The UV spectra and color of PMAA-*b*-PNIPAM-@-AuNPs (**a**) and PNIPAM-*b*-PMAA-@-AuNPs (**b**) at different temperature. Both hybrid particles were prepared by 0.01 wt% naked AuNPs conjugating with 0.01 mmol/L corresponding polymers at pH 7

SPR could be repeatedly cycled between redshift and recovery. After repeating several cycles, the location of SPR has a minor change, indicating that the AuNPs are effectively protected by grafting polymers during the process of aggregation-dispersion.

Temperature responsive properties of PMAA-b-PNIPAM-@-AuNPs and PNIPAM-b-PMAA-@-AuNPs The thermo-responsive behavior was also investigated by UV-Vis absorption spectroscopy. Both hybrid particles were subjected to the increasing temperature from 25 to 60 °C, and their absorption spectrum is shown in Fig. 7. From the Fig. 7, the position of maximum absorption of different temperature remains constant, but the intensity increases with rising temperature. However, the increment of absorption intensity of PNIPAM-b-PMAA-@-AuNPs (Fig. 7b) is obviously higher than that of PMAA-*b*-PNIPAM-@-AuNPs (Fig. 7a). The temperature response of corona layer strongly impacted the colloidal stability, which can be confirmed by the emergence of turbidity in the sample PNIPAM-b-PMAA-@-AuNPs at 60 °C (the inserted photo in Fig. 7b).

The temperature-dependent transmittance was detected at wavelength 600 nm to avoid interference of SPR. The transmittance of each hybrid particles is gradually reduced with rising temperature (Fig. 8). The same trend was also found in others report of thermo-responsive polymers monolayer protected AuNPs. For example, Beija prepared poly(*N*-vinyl caprolactam)-coated gold nanoparticles shown a violent aggregation and the sharp reduced transmittance to 1 % at high temperature [20]. However, the thermo-responsive block copolymer coated AuNPs exhibits a slight aggregation due to the space cooperation from the other block. The phase transition temperature of the PMAA-*b*-PNIPAM-@-AuNPs is 38 °C and that of PNIPAM-*b*-PMAA-@-AuNPs is 35 °C.

The TEM images of PMAA-*b*-PNIPAM-@-AuNPs and PNIPAM-*b*-PMAA-@-AuNPs at 40 °C are shown in Fig. 9. From Fig. 9a, the PMAA-*b*-PNIPAM-@-AuNPs exhibits a favorable dispersibility at high temperatures consistently with the results of UV-Vis spectroscopy (Fig. 7a). Similarly, smaller shrunk D_h (from 42 to 36 nm), the inserted image on Fig. 9a, indicates that inner PNIPAM shell turns to hydrophobic, but the particles remain a stable dispersion owing to the space and electrostatic protection of PMAA chains. On the contrary, the obvious aggregation is found in the PNIPAM-*b*-PMAA-@-AuNPs system (Fig. 9b). As the change of hydrophilic corona of PNIPAM chains to hydrophobic, the hybrid particles show a self-aggregation behavior, which also confirmed by a sharp increase D_h and widened particle distribution.

The thermo-responsive PNIPAM-*b*-PMAA-@-AuNPs can turn transparent when the temperature is reset to 25 °C. The

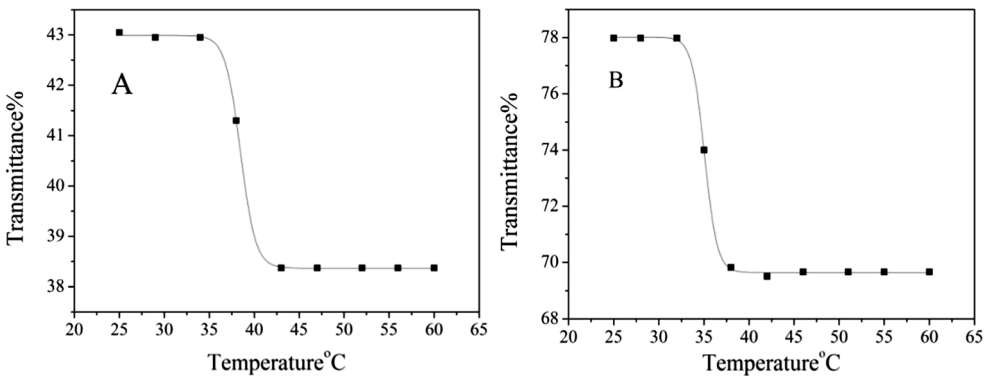

Fig. 8 Transmittance of PMAA-*b*-PNIPAM-@-AuNPs (**a**) and PNIPAM-*b*-PMAA-@-AuNPs (**b**) in aqueous solution from 25 to 60 °C. Both hybrid particles were prepared by 0.01 wt% naked AuNPs conjugating with 0.01 mmol/L corresponding polymers at the pH 7

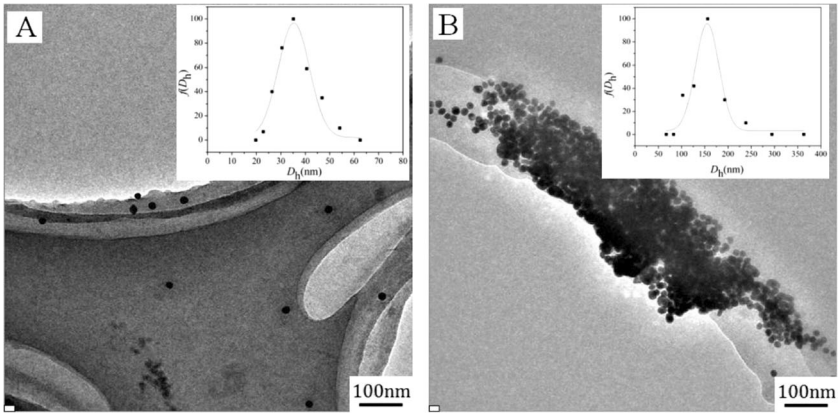

Fig. 9 TEM images of PMAA-*b*-PNIPAM-@-AuNPs (**a**) and PNIPAM-*b*-PMAA-@-AuNPs (**b**) at 40 °C

temperature-dependent clear-opaque transition is completely reversible. Figure 10 shows the response of optical transparency of the hybrid AuNPs with a thermo-responsive corona over several heat-cool cycles between 40 and 25 °C. Interestingly, the transition remained fully reversible over the six cycles tested. In the transition regime, the optical transparency, as a function of temperature, depends on the reversible conformation change of the PNIPAM corona upon thermal stimuli.

Conclusions

Two dual-stimuli responsive block copolymer protected gold nanoparticles, PMAA-*b*-PNIPAM-@-AuNPs and PNIPAM-*b*-PMAA-@-AuNPs, have been prepared by "grafting to" approach. The aggregation behaviors of the two hybrid AuNPs were found mainly to be affected by the phase transformation of the stimuli-responsive corona via changing pH or temperature of the aqueous medium, respectively. For PMAA-*b*-PNIPAM-@-AuNPs, the dispersibility of the hybrid AuNPs was determined by the PMAA blocks depending on the pH value of solution. Moreover, with the pH switching between 2.0 and 10.0, the SPR could be repeatedly cycled between redshift and recovery. However, the aggregation behavior and change of SPR affected by temperature were moderate owning to the protective effects of PMAA. For PNIPAM-*b*-PMAA-@-AuNPs, the PNIPAM reversibly induced the interparticles aggregation/dispersion process depending on the temperature of solution. The optical transparency of the hybrid AuNPs remained fully reversible over six heat-cool cycles with the temperatures above and below the LCST for the reversible conformation change of the corona. Correspondingly, at different pH, the hybrid AuNPs retained a stable dispersion with the hydrophilic PMAA turning to hydrophobic because of the space or electrostatic protection by PNIPAM. Overall, the obvious interparticle aggregation behaviors are caused by the phase transition for hydrophobic coronal polymer and the optical properties can be adjusted by changing temperature or pH of the solution.

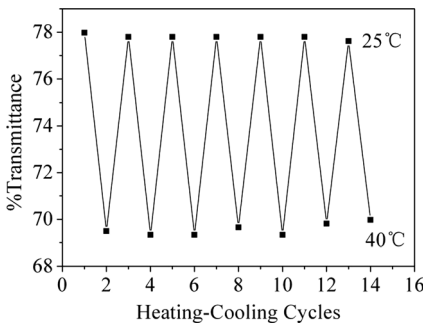

Fig. 10 Thermo-induced switching of transmittance of PNIPAM-*b*-PMAA-@-AuNPs with the temperatures above and below the LCST, where the solution was prepared by 0.01 wt% naked AuNPs conjugating with 0.01 mmol/L PNIPAM-*b*-PMAA at pH 7

Acknowledgement This work was supported by the National Natural Science Foundation of China (No.51103035) and Scientific & technological project of Henan Province (No.132102310422).

References

1. Rana S, Bajaj A, Mout R, Rotello VM (2012) Monolayer coated gold nanoparticles for delivery applications. Adv Drug Deliv Rev 64:200–216
2. Song YZ, Zhou JF, Song Y, Cheng ZP, Xu J (2012) Synthesis of netlike gold nanoparticles using ampicillin as a stabilizing reagent and its application. Mater Res Bull 47:4266–4270
3. Biswas M, Dinda E, Rashid MH, Mandal TK (2012) Correlation between catalytic activity and surface ligands of monolayer protected gold nanoparticles. J Colloid Interface Sci 368:77–85
4. Chen X, Zhao D, An Y, Shi L, Hou W, Chen L (2010) Catalytic properties of gold nanoparticles immobilized on the surfaces of nanocarriers. J Nanoparticle Res 12:1877–1887
5. Chen X, Zhao D, Zhao L, An Y, Ma R, Shi L, He Q, Chen L (2009) Optic and catalytic properties of gold nanoparticles tuned by homopolymers. Sci China Ser B-Chem 52:1372–1381
6. Chen X, Zhao D, An Y, Zhang Y, Cheng J, Wang B, Shi L (2008) Formation and catalytic activity of spherical composites with surfaces coated with gold nanoparticles. J Colloid Interface Sci 322:414–420

7. Chen X, An Y, Zhao D, He Z, Zhang Y, Cheng J, Shi L (2008) Core −shell−corona Au−micelle composites with a tunable smart hybrid shell. Langmuir 24:8198–8204
8. Kim D, Jon S (2012) Gold nanoparticles in image-guided cancer therapy. Inorg Chim Acta 393:154–164
9. Eshghi H, Sazgarnia A, Rahimizadeh M, Attaran N, Bakavoli M, Soudmand S (2013) Protoporphyrin IX—gold nanoparticle conjugates as an efficient photosensitizer in cervical cancer therapy. Photodiagn Photodyn Ther 10:304–312
10. Sun X, Zhang G, Keynton RS, O'Toole MG, Patel D, Gobin AM (2013) Enhanced drug delivery via hyperthermal membrane disruption using targeted gold nanoparticles with PEGylated protein-G as a cofactor. Nanomed: Nanotechnol Biol Med 9:1214–1222
11. Huang Y, Yu F, Park Y-S, Wang J, Shin M-C, Chung HS, Yang VC (2010) Co-administration of protein drugs with gold nanoparticles to enable percutaneous delivery. Biomaterials 31:9086–9091
12. Chai F, Wang CA, Wang TT, Li L, Su ZM (2010) Colorimetric detection of Pb2+ using glutathione functionalized gold nanoparticles. ACS Appl Mater Interfaces 2:1466–1470
13. Hung Y-L, Hsiung T-M, Chen Y-Y, Huang Y-F, Huang C-C (2010) Colorimetric Detection of Heavy Metal Ions Using Label-Free Gold Nanoparticles and Alkanethiols. J Phys Chem C 114:16329–16334
14. Zhang K, Cutler JI, Zhang J, Zheng D, Auyeung E, Mirkin CA (2010) Nanopod formation through gold nanoparticle templated and catalyzed cross-linking of polymers bearing pendant propargyl ethers. J Am Chem Soc 132:15151–15153
15. Oren R, Liang Z, Barnard JS, Warren SC, Wiesner U, Huck WTS (2009) Organization of nanoparticles in polymer brushes. J Am Chem Soc 131:1670–1671
16. Yavuz MS, Jensen GC, Penaloza DP, Seery TAP, Pendergraph SA, Rusling JF, Sotzing GA (2009) Gold nanoparticles with externally controlled, reversible shifts of local surface plasmon resonance bands. Langmuir 25:13120–13124
17. Grimm A, Nowak C, Hoffmann J, Schärtl W (2009) Electrophoretic mobility of gold nanoparticles in thermoresponsive hydrogels. Macromolecules 42:6231–6238
18. Parry AL, Clemson NA, Ellis J, Bernhard SSR, Davis BG, Cameron NR (2013) 'Multicopy Multivalent' glycopolymer-stabilized gold nanoparticles as potential synthetic cancer vaccines. J Am Chem Soc 135:9362–9365
19. Krieg A, Weber C, Hoogenboom R, Becer CR, Schubert US (2012) Block copolymers of poly(2-oxazoline)s and poly(meth)acrylates: a crossover between cationic ring-opening polymerization (CROP) and reversible addition–fragmentation chain transfer (RAFT). ACS Macro Lett 1:776–779
20. Beija M, Marty J-D, Destarac M (2011) Thermoresponsive poly(*N*-vinyl caprolactam)-coated gold nanoparticles: sharp reversible response and easy tunability. Chem Commun 47:2826–2828
21. Chakraborty S, Bishnoi SW, Pérez-Luna VH (2010) Gold nanoparticles with poly(*N*-isopropylacrylamide) formed via surface initiated atom transfer free radical polymerization exhibit unusually slow aggregation kinetics. J Phys Chem C 114:5947–5955
22. Qian X, Li J, Nie S (2009) Stimuli-responsive SERS nanoparticles: conformational control of plasmonic coupling and surface raman enhancement. J Am Chem Soc 131:7540–7541
23. Housni A, Zhao Y, Zhao Y (2010) Using polymers to photoswitch the aggregation state of gold nanoparticles in aqueous solution. Langmuir 26:12366–12370
24. Kairdolf BA, Nie S (2011) Multidentate-protected colloidal gold nanocrystals: pH control of cooperative precipitation and surface layer shedding. J Am Chem Soc 133:7268–7271
25. Gibson MI, O'Reilly RK (2013) To aggregate, or not to aggregate? Considerations in the design and application of polymeric thermally-responsive nanoparticles. Chem Soc Rev 42:7204–7213
26. Vogel N, Fernández-López C, Pérez-Juste J, Liz-Marzán LM, Landfester K, Weiss CK (2012) Ordered arrays of gold nanostructures from interfacially assembled Au@PNIPAM hybrid nanoparticles. Langmuir 28:8985–8993
27. Ignacio-de Leon PAA, Zharov I (2013) SiO2@Au core–shell nanospheres self-assemble to form colloidal crystals that can be sintered and surface modified to produce ph-controlled membranes. Langmuir 29:3749–3756
28. Lee H, Sample C, Cohen RE, Rubner MF (2013) pH-programmable sequential dissolution of multilayer stacks of hydrogen-bonded polymers. ACS Macro Lett 2:924–927
29. He J, Huang X, Li Y-C, Liu Y, Babu T, Aronova MA, Wang S, Lu Z, Chen X, Nie Z (2013) Self-assembly of amphiphilic plasmonic micelle-like nanoparticles in selective solvents. J Am Chem Soc 135:7974–7984
30. Chen T, Xu S, Zhao T, Zhu L, Wei D, Li Y, Zhang H, Zhao C (2012) Gold nanocluster-conjugated amphiphilic block copolymer for tumor-targeted drug delivery. ACS Appl Mater Interfaces 4:5766–5774
31. Hamner KL, Alexander CM, Coopersmith K, Reishofer D, Provenza C, Maye MM (2013) Using temperature-sensitive smart polymers to regulate dna-mediated nanoassembly and encoded nanocarrier drug release. ACS Nano 7:7011–7020
32. Nuopponen M, Tenhu H (2007) Gold nanoparticles protected with pH and temperature-sensitive diblock copolymers. Langmuir 23: 5352–5357
33. Banerjee R, Dutta S, Pal S, Dhara D (2013) Spontaneous formation of vesicles by self-assembly of cationic block copolymer in the presence of anionic surfactants and their application in formation of polymer embedded gold nanoparticles. J Phys Chem B 117:3624–3633
34. Zhao D, Chen X, Liu Y, Wu C, Ma R, An Y, Shi L (2009) Thermosensitive and pH-sensitive Au–Pd bimetallic nanocomposites. J Colloid Interface Sci 331:104–112
35. Storhoff JJ, Elghanian R, Mucic RC, Mirkin CA, Letsinger RL (1998) One-pot colorimetric differentiation of polynucleotides with single base imperfections using gold nanoparticle probes. J Am Chem Soc 120:1959–1964
36. Gehan H, Fillaud L, Chehimi MM, Aubard J, Hohenau A, Felidj N, Mangeney C (2010) Thermo-induced electromagnetic coupling in gold/polymer hybrid plasmonic structures probed by surface-enhanced raman scattering. ACS Nano 4: 6491–6500
37. Sardar R, Bjorge NS, Shumaker-Parry JS (2008) pH-controlled assemblies of polymeric amine-stabilized gold nanoparticles. Macromolecules 41:4347–4352
38. Nergiz SZ, Singamaneni S (2011) Reversible tuning of plasmon coupling in gold nanoparticle chains using ultrathin responsive polymer film. ACS Appl Mater Interfaces 3:945–951
39. Luo S, Xu J, Zhang Y, Liu S, Wu C (2005) Double hydrophilic block copolymer monolayer protected hybrid gold nanoparticles and their shell cross-linking. J Phys Chem B 109: 22159–22166
40. Raula J, Shan J, Nuopponen M, Niskanen A, Jiang H, Kauppinen EI, Tenhu H (2003) Synthesis of gold nanoparticles grafted with a thermoresponsive polymer by surface-induced reversible-addition-fragmentation chain-transfer polymerization. Langmuir 19:3499–3504
41. Eliassaf J, Silberberg A (1962) The gelation of aqueous solutions of polymethacrylic acid. Polymer 3:555–564
42. Olea AF, Thomas JK (1989) Fluorescence studies of the conformational changes of poly(methacrylic acid) with pH. Macromolecules 22:1165–1169
43. Mulvaney P (1996) Surface plasmon spectroscopy of nanosized metal particles. Langmuir 12:788–800
44. Noguez C (2007) Surface plasmons on metal nanoparticles: the influence of shape and physical environment. J Phys Chem C 111: 3806–3819